

On the Spin of the $X(3872)$

R. Faccini*, F. Piccinini†, A. Pilloni* and A.D. Polosa*

**Dipartimento di Fisica and INFN, ‘Sapienza’ Università di Roma,
Piazzale A. Moro 2, Roma, I-00185, Italy*

†INFN Pavia, Via A. Bassi 6, Pavia, I-27100, Italy

Whether the much studied $X(3872)$ is an axial or tensor resonance makes an important difference to its interpretation. A recent paper by the BaBar collaboration [1] raised the viable hypothesis that it might be a $J^{PC} = 2^{-+}$ state based on the $\pi^+\pi^-\pi^0$ spectrum in the $X \rightarrow J/\psi \omega$ decays. Furthermore, the Belle collaboration published the $\pi^+\pi^-$ invariant mass and spin-sensitive angular distributions in $X \rightarrow J/\psi \rho$ decays [2].

Starting from a general parametrization of the decay amplitudes for the axial and tensor quantum numbers of the X , we re-analyze the whole set of available data. The level of agreement of the two spin hypotheses with data is interpreted with a rigorous statistical approach based on Monte Carlo simulations in order to be able to combine all the distributions regardless of their different levels of sensitivity to the spin of the X .

Our analysis returns a probability of 5.5% and 0.1% for the agreement with data of the 1^{++} and 2^{-+} hypotheses, respectively, once we combine the whole information (angular and mass distributions) from both channels. On the other hand, the separate analysis of $J/\psi \rho$ (angular and mass distributions) and $J/\psi \omega$ (mass distribution) indicates that the 2^{-+} assignment is excluded at the 99.9% C.L. by the former case, while the latter excludes at the same level the 1^{++} hypothesis. There are therefore indications that the two decay modes behave in a different way.

PACS: 13.25.Ft, 14.40.Rt

I. INTRODUCTION

Although the $X(3872)$ resonance is the most studied among the exotic XYZ states, since its discovery in 2003, its quantum numbers have not been definitively identified yet.

The CDF collaboration concluded from the analysis of the angular distributions and correlations of the X decay products that the possible quantum numbers are $J^{PC} = 1^{++}$ or 2^{-+} [3]. Similar results have been found very recently by the BELLE collaboration [2]. In the latter paper the $\pi^+\pi^-$ invariant mass distribution is analyzed under the 1^{++} and 2^{-+} hypotheses, finding preference for the former whereas no preferred assignment emerges if an interfering contribution with the isospin-violating decay $\omega \rightarrow \pi^+\pi^-$ is added to the amplitude.

The picture becomes more puzzling as one considers the analysis by the BaBar Collaboration of the decay $X \rightarrow J/\psi \pi^+\pi^-\pi^0$ [1]. The expected 3π invariant mass distribution agrees with data slightly better if the 2^{-+} signature is assumed. This result on the 3π spectrum was later confirmed in [4].

In a recent paper [5] the pion invariant masses in the decays $X \rightarrow J/\psi 2\pi$ and $X \rightarrow J/\psi 3\pi$ are simultaneously analyzed with a combined fit, concluding that present data favor the 1^{++} assignment. In our view, the 2π invariant mass distribution is not able to resolve the two hypotheses despite of the high statistics, and the way the fit was performed leads to the dilution of the sensitivity of the 3π channel.

To improve the analysis of all available data sensitive to the spin of the X *i)* we write the decay matrix elements for both the 1^{++} and 2^{-+} hypotheses as given by enforcing Lorentz invariance and parity considerations, *ii)* we give a functional dependency on the decay momenta to the couplings introducing a length scale R – which is to be related to the finite size of the hadrons participating to the interactions, *iii)* we use the matrix elements of ρ and ω decays to take into account the appropriate decay waves; we do not pursue the Blatt-Weisskopf description as we find that all spin structure can appropriately be taken into account with no further approximations, *iv)* we perform a global fit to exploit the information contained in all the distributions available and we adopt a statistical approach appropriate when distributions with different sensitivities to the parameters of interest are combined.

II. MATRIX ELEMENTS

The matrix elements describing the amplitudes $X \rightarrow J/\psi V$ (where $V = \rho, \omega$) are obtained by Lorentz, gauge invariance and parity considerations leading to the formulae reported below [4].

In the $X(1^{++})$ case we have

$$\langle \psi(\epsilon, p) V(\eta, q) | X(\lambda, P) \rangle = g_{1\psi V} \epsilon^{\mu\nu\rho\sigma} \lambda_\mu(P) \epsilon_\nu^*(p) \eta_\rho^*(q) P_\sigma \quad (1)$$

the polarization vectors carry a complex conjugation when referred to final states.

In the 2^{-+} case we have a more complicated structure

$$\langle \psi(\epsilon, p) V(\eta, q) | X(\pi, P) \rangle = g_{2\psi V} T_A + g'_{2\psi V} T_B \quad (2)$$

where π is the polarization tensor for a spin two particle with mass¹ and a standard notation is used for the remaining polarization vectors. We find that T_A and T_B are given by

$$T_A = \epsilon^{*\alpha}(p) \pi_{\alpha\mu}(P) \epsilon^{\mu\nu\rho\sigma} p_\nu q_\rho \eta_\sigma^*(q) - (\epsilon, p \leftrightarrow \eta, q) \quad (4)$$

and

$$T_B = Q^\alpha \pi_{\alpha\mu}(P) \epsilon^{\mu\nu\rho\sigma} P_\nu \epsilon_\rho^*(p) \eta_\sigma^*(q) \quad (5)$$

where $Q = p - q$ and $P = p + q$.

The coupling $g_{1\psi V}$ is real whereas the couplings $g_{2\psi V}$ and $g'_{2\psi V}$ are separately real but can have a complex relative phase. This is due to the fact that, on the basis of Lorentz invariance and parity conservation, we can indeed write three terms $T_A^{(\lambda)}$, $T_B^{(\lambda)}$ and $T_C^{(\lambda)}$ where λ labels one out of the $3 \times 3 \times 5$ polarization combinations which define T_A, T_B, T_C . T_C is the same as T_A but with a plus relative sign between the two terms on the rhs of (4). Only two out of these three terms are linearly independent (say T_A and T_B) for

$$\left| \sum_{\lambda=1}^{3 \times 3 \times 5} T_A^{(\lambda)} T_C^{(\lambda)*} \right|^2 = \sum_{\lambda} |T_A^{(\lambda)}|^2 \sum_{\lambda} |T_C^{(\lambda)}|^2 \quad (6)$$

which is the equality of the Schwartz inequality: this holds if $z_1 T_A = z_2 T_C$ where z_1 and z_2 are two complex numbers both different from zero. Thus we can exclude T_C and retain T_B and, in general, $z_1 T_A$ to characterize the decay amplitude.

In Refs. [1, 2, 5] the P -wave fit functions contain a Blatt-Weisskopf angular momentum barrier factor of the form $(1 + R^2 q^{*2})^{-1/2}$, where q^* is the X decay 3-momentum. The value of R cannot be extracted from data since the P -wave distribution will approach the S -wave distribution in the limit $R \rightarrow \infty$, so that if we let R free, the fit will not converge. On the other hand, in our discussion we do not need any barrier factor the decay wave being dictated by the expressions of the matrix elements. We instead take into account the finite size of the X (and of V and J/ψ as well) introducing a ‘polar’ form factor, namely

$$g \rightarrow \frac{g}{(1 + R^2 q^{*2})^n} \quad (7)$$

where g stands in general for $g_{1\psi V}$, $g_{2\psi V}$ and $g'_{2\psi V}$. We tested the values $n = 1$ and $n = 2$ (the latter coinciding with the Fourier transform of a an exponential $g(r) \sim \exp(-r/R)$ strong charge distribution). Both the fitting functions turn out to be rather effective at improving our results, with no significative change for the the two choices of n . We also underscore that $g_{1\psi V}$ (regulating the S -wave decay) is assumed to have the same polar behavior since Eq. (7) does not concern any orbital angular momentum considerations. The size parameters R_J will eventually be fitted from data.

As for the ρ and ω decay amplitudes, we use

$$\langle \pi^+(p) \pi^-(q) | \rho(\epsilon, P) \rangle = g_{\rho 2\pi} \epsilon \cdot p \quad (8)$$

which describes a P -wave decay (the square modulus of this matrix element is $g_{\rho 2\pi}^2$ times the decay momentum squared). For the ω we have

$$\langle \pi^+(p) \pi^-(q) \pi^0(r) | \omega(\epsilon, P) \rangle = g_{\omega 3\pi} \epsilon^{\mu\nu\rho\sigma} \epsilon_\mu p_\nu q_\rho r_\sigma \quad (9)$$

The last two couplings will simply be written in terms of the partial widths $\Gamma(\rho \rightarrow 2\pi)$ and $\Gamma(\omega \rightarrow 3\pi)$, as shown in the next section.

¹ The sum over polarizations is

$$\sum_{\text{pol}} \pi_{\mu\nu}(k) \pi_{\alpha\beta}^*(k) = \frac{1}{2} T_{\mu\alpha} T_{\nu\beta} + \frac{1}{2} T_{\mu\beta} T_{\nu\alpha} - \frac{1}{3} T_{\mu\nu} T_{\alpha\beta} \quad (3)$$

with $T_{\mu\nu} = -g_{\mu\nu} + k_\mu k_\nu / m^2$ and $k^2 = m^2$.

III. DECAY WIDTHS

We have to calculate the partial widths $\Gamma(X \rightarrow J/\psi \pi^+ \pi^-)$ and $\Gamma(X \rightarrow J/\psi \pi^+ \pi^- \pi^0)$. In what follows we will neglect the ρ - ω mixing since we demonstrate in Appendix A that it does not alter significantly the results. The partial widths in the narrow width approximation are [4]

$$\begin{aligned} \Gamma(X \rightarrow J/\psi \pi^+ \pi^-) &= \frac{1}{2J+1} \frac{1}{48\pi m_X^2} \int ds \sum_{\text{pol}} |\langle \psi \rho(s) | X \rangle|^2 p^*(m_X^2, m_\psi^2, s) \\ &\times \frac{1}{\pi} \frac{1}{(s - m_\rho^2)^2 + (m_\rho \Gamma_\rho)^2} \int d\Phi^{(2)} \sum_{\text{pol}} |\langle \pi^+ \pi^- | \rho(s) \rangle|^2 \end{aligned} \quad (10)$$

where by $d\Phi^{(2)}$ we mean the 2-body phase space measure. The decay momentum q^* in the matrix element $\langle \psi \rho(s) | X \rangle$ coincides with $q^* \equiv p^*(m_X^2, m_\psi^2, s)$; similarly for the width in $J/\psi \omega$ discussed below.

The sum over polarizations in (8), simply yields

$$\sum_{\text{pol}} |\langle \pi^+ \pi^- | \rho(s) \rangle|^2 = g_{\rho 2\pi}^2 p^*(s, m_\pi^2, m_\pi^2)^2 \quad (11)$$

Finally, we can eliminate the coupling by evaluating the (11) on the mass-shell and by relating it to the partial width $\Gamma(\rho \rightarrow \pi\pi)$

$$g_{\rho 2\pi}^2 = 6m_\rho^2 \Gamma(\rho \rightarrow \pi\pi) \frac{4\pi}{p^*(m_\rho^2, m_\pi^2, m_\pi^2)^3} \quad (12)$$

Inserting the above expressions (11), (12) into (10) gives

$$\begin{aligned} \Gamma(X \rightarrow J/\psi \pi^+ \pi^-) &= \frac{1}{2J+1} \frac{1}{8\pi m_X^2} \int ds \sum_{\text{pol}} |\langle \psi \rho(s) | X \rangle|^2 p^*(m_X^2, m_\psi^2, s) \\ &\times \frac{1}{\pi} \frac{m_\rho \Gamma_\rho \mathcal{BR}(\rho \rightarrow \pi\pi)}{(s - m_\rho^2)^2 + (m_\rho \Gamma_\rho)^2} \frac{m_\rho}{\sqrt{s}} \left(\frac{p^*(s, m_\pi^2, m_\pi^2)}{p^*(m_\rho^2, m_\pi^2, m_\pi^2)} \right)^3 \end{aligned} \quad (13)$$

Similarly, for the ω we obtain

$$\begin{aligned} \Gamma(X \rightarrow J/\psi \pi^+ \pi^- \pi^0) &= \frac{1}{2J+1} \frac{1}{48\pi m_X^2} \int ds \sum_{\text{pol}} |\langle \psi \omega(s) | X \rangle|^2 p^*(m_X^2, m_\psi^2, s) \\ &\times \frac{1}{\pi} \frac{1}{(s - m_\omega^2)^2 + (m_\omega \Gamma_\omega)^2} \int d\Phi^{(3)} \sum_{\text{pol}} |\langle \pi^+ \pi^- \pi^0 | \omega(s) \rangle|^2 \end{aligned} \quad (14)$$

Summing over the ω polarizations

$$\sum_{\text{pol}} |\langle \pi^+ \pi^- \pi^0 | \omega(s) \rangle|^2 = \frac{g_{\omega 3\pi}^2}{s^3} \frac{s}{4} [(m_0^2 + s - 2\sqrt{s}\omega)(\omega^2 - m_0^2 - 4x^2) - 4m_+^2(\omega^2 - m_0^2)] \equiv g_{\omega 3\pi}^2 \mathcal{M}(\sqrt{s}) \quad (15)$$

where $\omega = E_{\pi^0}$, $x = \frac{1}{2}(E_{\pi^+} - E_{\pi^-})$ and $m_0 = m_{\pi^0}$, $m_+ = m_{\pi^+} = m_{\pi^-}$. An adimensional coupling has been formed by substituting $g_{\omega 3\pi}^2 \rightarrow \frac{1}{s^3} g_{\omega 3\pi}^2$ ². We eliminate the coupling by evaluating (15) on the mass-shell

$$g_{\omega 3\pi}^2 = 6m_\omega \Gamma(\omega \rightarrow 3\pi) \left(\int d\Phi^{(3)} \mathcal{M}(m_\omega) \right)^{-1} \quad (16)$$

² This rescaling is arbitrary and in part relies on the narrowness of the ω . Avoiding the introduction of the $1/s^3$ term, the separate fit of 3π does not change significantly (for example, with $n = 1$, the 2^{--} is unchanged, the 1^{++} gets worse from $\chi^2 = 9.9 \rightarrow 11.1$). In the combined fit of invariant mass distributions both hypotheses become a bit worse (again for $n = 1$, 2^{--} : $\chi^2 = 17.7 \rightarrow 18.4$; 1^{++} : $\chi^2 = 25.2 \rightarrow 26.2$) so that the $\Delta\chi^2$ remains almost unchanged. See Sec. IV A.

Inserting (15), (16) into (14) we obtain

$$\begin{aligned} \Gamma(X \rightarrow J/\psi \pi^+ \pi^- \pi^0) &= \frac{1}{2J+1} \frac{1}{8\pi m_X^2} \int ds \sum_{\text{pol}} |\langle \psi \omega(s) | X \rangle|^2 p^*(m_X^2, m_\psi^2, s) \\ &\times \frac{1}{\pi} \frac{m_\omega \Gamma_\omega \mathcal{BR}(\omega \rightarrow 3\pi)}{(s - m_\omega^2)^2 + (m_\omega \Gamma_\omega)^2} \frac{\Phi^{(3)'}(\sqrt{s}, m_0, m_+, m_+)}{\Phi^{(3)'}(m_\omega, m_0, m_+, m_+)} \end{aligned} \quad (17)$$

where

$$\Phi^{(3)'}(\sqrt{s}, m_0, m_+, m_+) = \frac{1}{32\pi^3} \int_{m_0}^{\omega_m} d\omega \int_{x_-}^{x_+} dx \frac{1}{4s^2} [(m_0^2 + s - 2\sqrt{s}\omega)(\omega^2 - m_0^2 - 4x^2) - 4m_+^2(\omega^2 - m_0^2)] \quad (18)$$

with $\omega_m = (m_0^2 - 4m_+^2 + s)/(2\sqrt{s})$ and

$$x_\pm = \pm \frac{1}{2} \sqrt{\frac{(\omega^2 - m_0^2)(\omega_m - \omega)\sqrt{s}}{4m_+^2 + (\omega_m - \omega)\sqrt{s}}} \quad (19)$$

to be compared to the notations used in [4].

In formulae (13) and (17) angular correlations are not taken into account for we factorize matrix elements. On the other hand, the only way to consider both off-shellness and angular correlations is to compute the full matrix element for the $1 \rightarrow 5$ decay

$$\begin{aligned} \Gamma(B \rightarrow K X \rightarrow K J/\psi \rho \rightarrow K l^+ l^- \pi^+ \pi^-) &= \frac{1}{2m_B} \int \prod_{i=1}^5 \frac{d^3 p_i}{(2\pi)^3 2E_i} (2\pi)^4 \delta\left(p_B - \sum_i p_i\right) \\ &\times \sum_{\text{pol}} |\langle K l^+ l^- \pi^+ \pi^- | B \rangle|^2 \end{aligned} \quad (20)$$

The matrix element can be decomposed as

$$\begin{aligned} \langle K l^+ l^- \pi^+ \pi^- | B \rangle &= \langle l^+ l^- | \psi \rangle \frac{1}{p_\psi^2 - m_\psi^2 + im_\psi \Gamma_\psi} \langle \pi^+ \pi^- | \rho \rangle \frac{1}{p_\rho^2 - m_\rho^2 + im_\rho \Gamma_\rho} \\ &\times \langle \psi \rho | X \rangle \frac{1}{p_X^2 - m_X^2 + im_X \Gamma_X} \langle K X | B \rangle \end{aligned} \quad (21)$$

We already gave a form to $\langle \psi \rho | X \rangle$ and $\langle \pi^+ \pi^- | \rho \rangle$ in Sec. II for both 1^{++} and 2^{-+} . Moreover

$$\langle l^+ l^- | \psi \rangle = (\epsilon_\psi)_\beta \bar{u}(l^-) \gamma^\beta v(l^+) \quad (22)$$

$$\langle \pi^+ \pi^- | \rho \rangle = \epsilon_\rho \cdot p_{\pi^+} \quad (23)$$

$$\langle X K | B \rangle = \begin{cases} \epsilon_X^* \cdot p_K & \text{for } 1^{++} \\ (\pi_X^*)_{\delta\varphi} (p_K)^\delta (p_K)^\varphi & \text{for } 2^{-+} \end{cases} \quad (24)$$

The sum over polarizations of inner legs returns the usual numerators of spin-1 and spin-2 propagators. The expressions obtained are not reported here because of their algebraic complexity³. All matrix elements but the $\langle \psi \rho | X(2^{-+}) \rangle$ can be written in terms of one coupling only times a scalar function of momenta and polarizations.

The widths are expressed in terms of sums of products of couplings times scalar functions of momenta. Products of couplings are absorbed within the fit parameters τ_j^{ang} see Sec. IV.

Since the integral in Eq. (20) has to be evaluated numerically, we use Monte Carlo techniques. The integration on the 5-body phase space is carried out using importance sampling on the Breit-Wigner peaks. As a further option of the calculation, unweighted decay configurations can be generated according to full matrix element weights.

As usual, in the calculations we use the so-called *comoving width*, i.e. we rescale the width in the denominators of Eqs. (13), (17) and (21) according to the standard prescription $m\Gamma \rightarrow (s/m)\Gamma$.

³ These are available upon request in form of Fortran routines.

IV. DATA RE-ANALYSIS

In order to extract information on the spin of the X particle, we re-analyze the $B \rightarrow XK$ data published in Ref. [2] (for $X \rightarrow J/\psi \pi^+ \pi^-$) and in Ref. [1] (for $X \rightarrow J/\psi \pi^+ \pi^- \pi^0$). In particular, in the $X \rightarrow J/\psi \pi^+ \pi^-$ sample we consider the di-pion invariant mass ($m_{2\pi}$) and the angles defined in the X rest frame in Ref. [7] and described in Fig 1: the angle between the J/ψ and the direction opposite to K (θ_X), the angle between the π^+ and the direction opposite to K (χ), and the angle between the l^+ produced by the decay of the J/ψ and the z -axis of a coordinate system where the x -axis is the direction opposite to the K and the y -axis is the component of π^+ orthogonal to K (θ_l). In the $X \rightarrow J/\psi \pi^+ \pi^- \pi^0$, instead, only the three pions invariant mass is considered ($m_{3\pi}$).

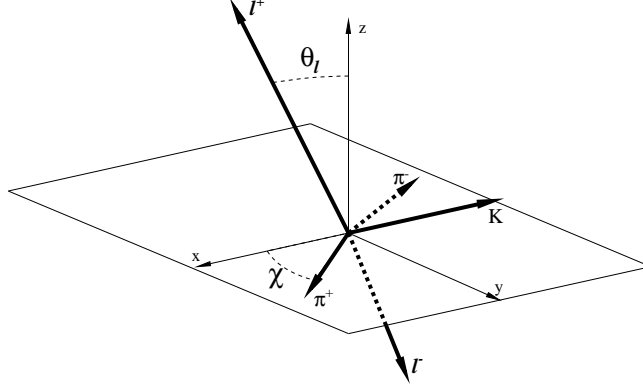


FIG. 1: Definition of the angles in $X \rightarrow J/\psi \pi^+ \pi^-$ [2].

With such distributions at hand the parameters of the model we have sensitivity upon are

- the radii R_J ($J = 1, 2$) as defined in Eq. (7), to which only the invariant mass distributions are sensitive
- the relative amplitudes and phases of the two contributions in case $J = 2$ ($g_{2\psi V}$ and $g'_{2\psi V}$ in Eq. (2)). We redefine

$$g_{2\psi\xi} = r_{2\xi} \cos \frac{\theta_\xi}{2}, \quad g'_{2\psi\xi} = r_{2\xi} \sin \frac{\theta_\xi}{2} e^{i\varphi_\xi} \quad (25)$$

where ξ can be ρ , ω or ang, depending on whether we are fitting the $m_{2\pi}$, $m_{3\pi}$, or angular distributions respectively. The parameters θ_ρ and φ_ρ satisfy $\theta_\rho = \theta_{\text{ang}}$ and $\varphi_\rho = \varphi_{\text{ang}}$ since in the ρ channel we have information on both mass spectrum and angular distributions. Only the angular distributions are sensitive to the θ and φ parameters

- the overall normalizations, $r_{2\xi}$ and $r_{1\xi}$ ($= g_{1\psi\rho}$ in Eq. ((1))). It has to be noted that the normalization depends on the distributions being studied

Given the different sensitivities of the mass and angle distributions and the computational complexity of the angular fits, the combined fits are performed in three steps: *i*) the invariant mass distributions are fitted letting all parameters float, *ii*) the fits to the three angular distributions are performed fixing the R_J parameters to the results obtained in the previous fits, *iii*) the invariant mass fits are repeated by fixing the θ_ρ and φ_ρ distributions to the results of the angular fits. φ_ω and θ_ω are always set to zero.

Mass and widths of the ρ , ω , and X are fixed. To account for the X width in the invariant mass distributions, we extract randomly the values of the mass of the X from a Breit-Wigner centered at $m_X = 3872 \text{ MeV}$ with $\Gamma_X = 1.7 \text{ MeV}$ [8], accepting only those values kinematically consistent with the decay of interest.

Finally, since as described in Appendix B the invariant mass fits return consistent results with either the $n = 1$ or the $n = 2$ hypotheses (where n is defined in Eq. (7)) we will only report results with $n = 1$.

The resulting fits are shown in Figs. 2 and 3 and the fitted parameters are summarized in Tab. I. It is interesting to note that the radii, which are the fit parameters with a physical content, have reasonably small errors and get values consistent with 1 fm, the size scale of a standard hadron. Here it is hard to judge if we are

probing the size of the X , in which case we would say that the results obtained for R disfavor a large (~ 10 fm) loosely bound molecule [9], or the size of the interaction making the X decay into $J/\psi + V$. For sure the loosely bound molecule is requested to have a large wave function at the origin to make such a decay possible ⁴. On the other hand in any compact multiquark model the decay into J/ψ does not require special conditions.

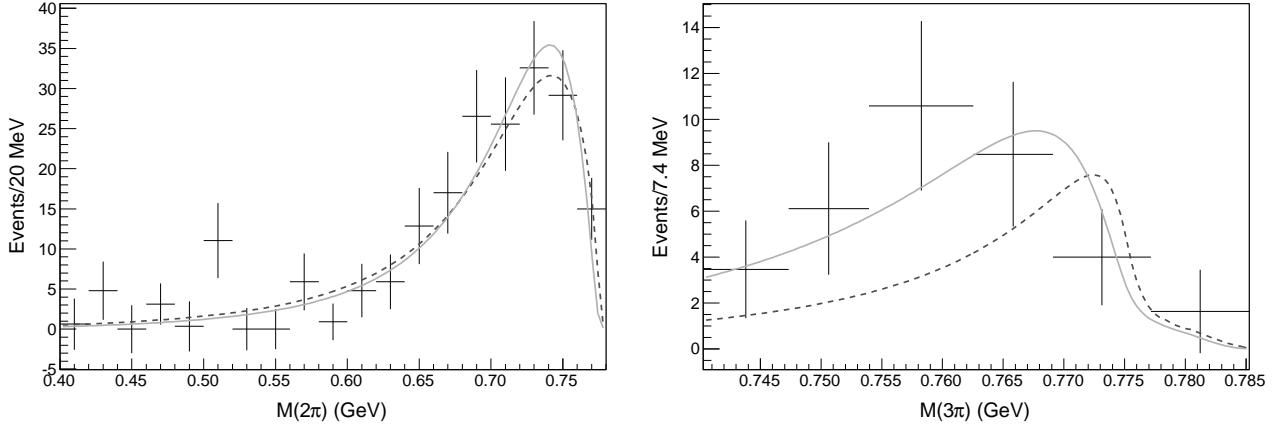


FIG. 2: Fit to the $m_{2\pi}$ (left) and $m_{3\pi}$ (right) distributions as described in the text, with the $n = 1$ model. The dashed curve refers to the 1^{++} hypothesis whereas the solid one is for the 2^{-+} .

A. Statistical interpretation

The naïve approach to evaluate the likelihood of the two spin hypotheses would be to consider the χ^2 of the fits, obtained by adding the contributions from all the distributions, and to compare them with the number of degrees of freedom. In our case this would return a $\chi^2/\text{DOF} = 31.8/36$ for the 1^{++} hypothesis and $\chi^2/\text{DOF} = 37.3/33$ for the 2^{-+} hypothesis. The probability of obtaining a worse value is $P(\chi^2) = \int_{\chi^2}^{\infty} \text{PDF}(x, N_{\text{DOF}}) dx = 67\%$ and 28% respectively, *i.e.*, both hypotheses seem to fit data well.

Nonetheless this conclusion would not consider two effects. First, the overall good agreements is caused by the fact that we are simultaneously considering the distributions which favor the 1^{++} hypothesis (θ_X, χ, θ_l) and the one which favors the 2^{-+} hypothesis ($m_{3\pi}$). This can be qualitatively seen in the fit results (Figs. 2 and 3) and in the $P(\chi^2)$ values obtained on each fitted distribution as listed in Tab. II. Then, a large number of degrees

	1^{++} (dashed curve)	2^{-+} (solid curve)
$r_{J\rho}$	0.089 ± 0.006 a.u.	0.69 ± 0.13 a.u.
$r_{J\omega}$	0.0026 ± 0.0003 a.u.	0.030 ± 0.016 a.u.
$r_{J\text{ang}}$	1.32 ± 0.4 a.u.	1.03 ± 0.04 a.u.
θ_ρ	-	$(254 \pm 16)^\circ$
φ_ρ	-	$(14 \pm 60)^\circ$
R_J	$1.6 \pm 0.3 \text{ GeV}^{-1}$	$5.6 \pm 0.8 \text{ GeV}^{-1}$
χ^2/DOF	31.8/36	37.3/33
$P(\chi^2)$	67%	28%

TABLE I: Fit results for the two J^{PC} assignments.

⁴ Moreover we remind that loosely bound molecules are very difficult to be produced with high cross sections at hadron colliders [10] if not invoking final state interactions effect [11].

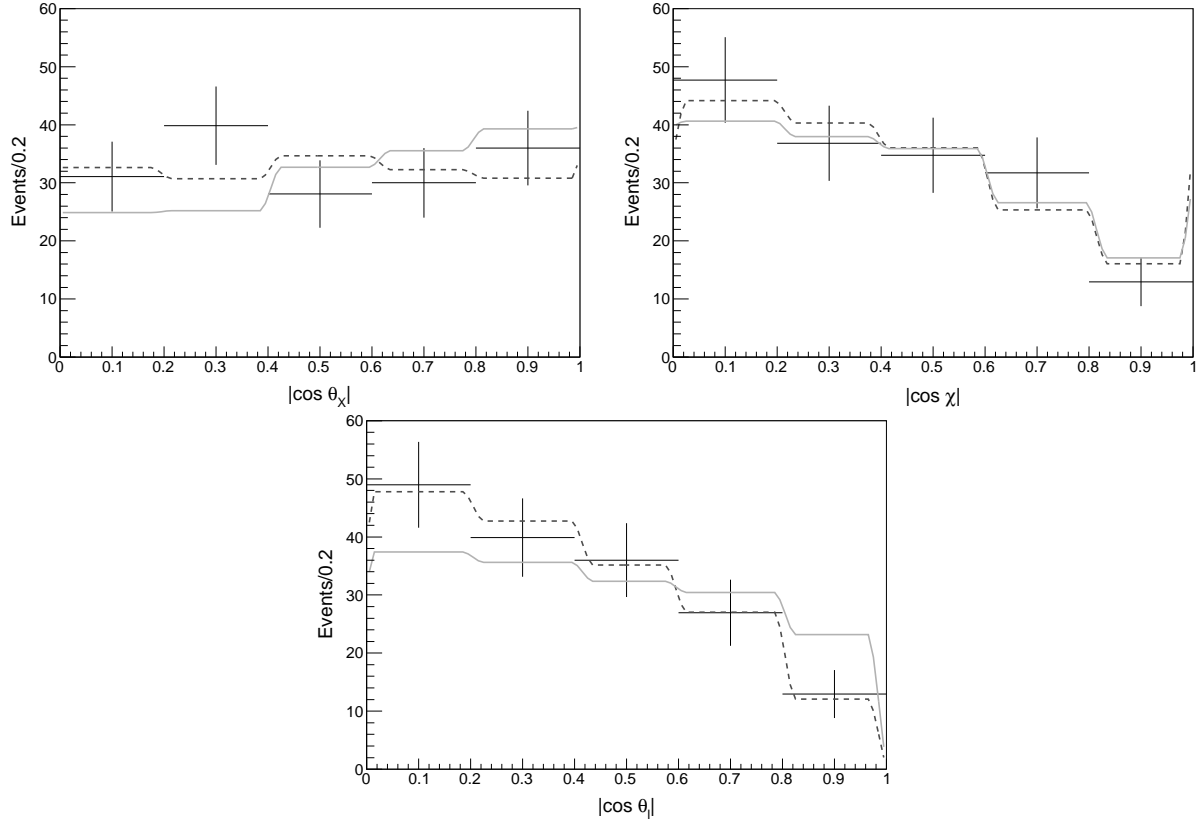


FIG. 3: Fit to the angular distributions in $X \rightarrow J/\psi \pi^+ \pi^-$ decays as described in the text. The dashed curve refers to the 1^{++} hypothesis whereas the solid one is for the 2^{-+} .

of freedom are not sensitive to the spin of the X and therefore wash out the overall χ^2 . This is the case for the $m_{2\pi}$ distribution, which is sensitive only to the radii, but not to the spin.

To quantify this latter statement and develop a sounder statistical analysis, we performed a Monte Carlo (MC) study. We generate N data samples with the same number of events as the experimental samples and take into account the background, the statistical fluctuations, and the uncertainties in the model parameters. The simulations can be performed either by making the hypothesis that the X is truly a 1^{++} state or a 2^{-+} state.

As the starting point of the simulation for a given J and n hypothesis we take the corresponding model extracting sample by sample the parameters according to the result of the combined fit to the data. The invariant mass MC samples are generated by filling the bins b_i according to Poisson distributions with mean values μ_i corresponding, bin per bin, to the sum of the values expected from the model and the experimental background. The angular pseudodata are generated as MC unweighted events.

After the extraction this background is treated in the same way as the data, subtracted in the case of the invariant mass distributions and accounted for in the fits in the case of the angular distributions.

The N data samples obtained with this procedure are then analyzed with the same fitting function and statistical analysis as the experimental data.

With such a tool, we first show the $P(\chi^2)$ values obtained on the $m_{2\pi}$ fits (Fig. 4) performed by generating the MC events with both the spin hypotheses and by fitting them either with the correct or the wrong hypothesis. These figures show that even when fitting with the incorrect X spin the fit would return a good $P(\chi^2)$. We therefore conclude that $m_{2\pi}$ is not sensitive to the X spin.

Since we need the invariant mass distributions to perform the combined fit to constraint the R_J variables, we developed a more robust method of testing the hypotheses by using as estimator the difference between the χ^2 obtained from the combined fits performed under the two J hypotheses [12]

$$\Delta\chi^2 = \chi^2(1^{++}) - \chi^2(2^{-+}) \quad (26)$$

Fig. 5 shows that the distribution of such a variable is peaked around a negative value when the MC samples

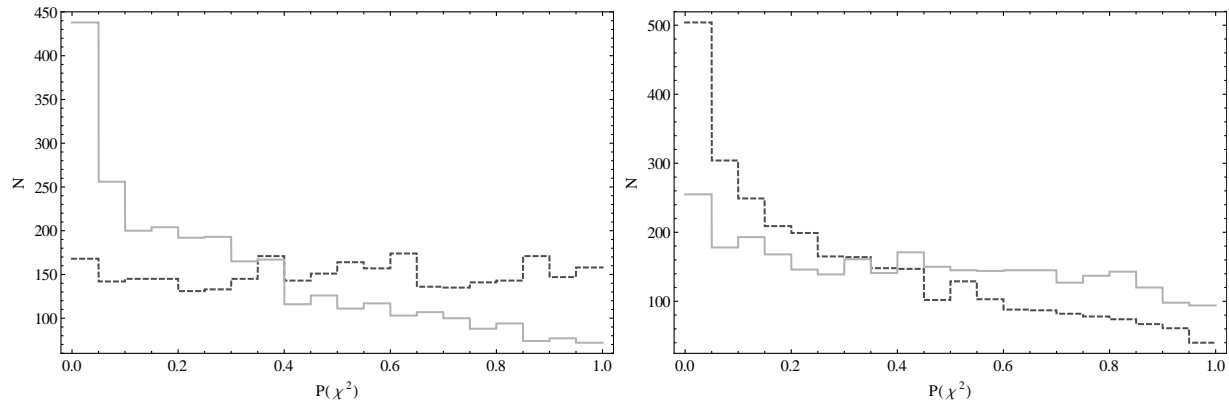


FIG. 4: Distribution of the $P(\chi^2)$ resulting from the fits to $m_{2\pi}$ in MC samples generated assuming 1^{++} (left) and 2^{-+} (right). The solid (dashed) histogram corresponds to the fit to the 2^{-+} (1^{++}) model.

are generated with 1^{++} and, viceversa, it is peaked around a positive value when the samples are generated with 2^{-+} . These distributions are used to calculate the fraction of samples in which $\Delta\chi^2$ has a value larger (for 1^{++}) or smaller (for 2^{-+}) than the one obtained on data. This fraction, that we call CL, estimates the probability of the hypothesis.

Given that in the combined fit $\Delta\chi^2 = -5.5$, the 2^{-+} hypothesis is excluded at 99.9% C.L., while the 1^{++} hypothesis has a C.L. of 5.5%. The different conclusion with respect to the naïve expectations is due to the fact that individual χ^2 values account only for the agreement of the data with the specific hypothesis under test. The $\Delta\chi^2$ approach instead also considers the level of agreement with the other hypothesis, weighting the degrees of freedom with their power to discriminate among the two hypotheses.

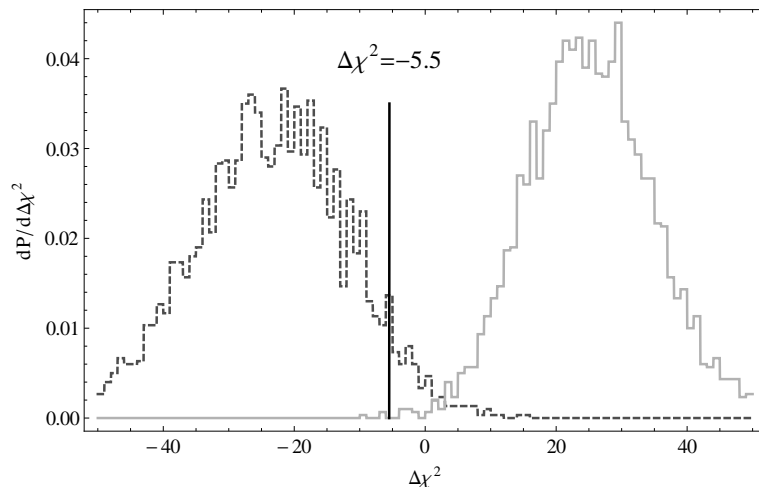


FIG. 5: Distribution of the $\Delta\chi^2 = \chi^2(1^{++}) - \chi^2(2^{-+})$ resulting from the combined fits to Monte Carlo data samples with $n = 1$. The solid (dashed) histogram corresponds to events generated assuming the X to be a 2^{-+} (1^{++}) state.

We mark with a line the position of the experimental $\Delta\chi^2$.

B. Fits on sub-samples

The $\Delta\chi^2$ interpretation of the combined fit shows that even the agreement of the data with the 1^{++} hypothesis is marginal and the fit results seem to hint that the disagreement concentrates in the $m_{3\pi}$ distribution (see Fig. 2). To quantify this statement we have performed the toy MC analysis on the $\Delta\chi^2$ value obtained separately on the $m_{3\pi}$ distribution (obtained on the $X \rightarrow J/\psi \pi^+\pi^-\pi^0$ sample) and on the combination of the other distributions (obtained on the $X \rightarrow J/\psi \pi^+\pi^-$ sample). The results, listed in Tab. II, show that the fits to the $X \rightarrow J/\psi \pi^+\pi^-$ distributions (second row) exclude the 2^{-+} hypothesis and have an agreement with the 1^{++}

	1^{++} (dashed curve)	2^{-+} (solid curve)
combined	$\chi^2/\text{DOF} = 31.8/36$ $P(\chi^2) = 67\%$ $CL = 5.5\%$	$\chi^2/\text{DOF} = 37.3/33$ $P(\chi^2) = 28\%$ $CL = 0.1\%$
2π (angular + mass)	$\chi^2/\text{DOF} = 20.9/31$ $P(\chi^2) = 91\%$ $CL = 23\%$	$\chi^2/\text{DOF} = 34.7/29$ $P(\chi^2) = 21\%$ $CL < 0.1\%$
3π (mass)	$\chi^2/\text{DOF} = 9.9/4$ $P(\chi^2) = 4\%$ $CL = 0.1\%$	$\chi^2/\text{DOF} = 1.5/3$ $P(\chi^2) = 68\%$ $CL = 81\%$
combined (only mass)	$\chi^2/\text{DOF} = 25.2/22$ $P(\chi^2) = 29\%$ $CL = 0.1\%$	$\chi^2/\text{DOF} = 17.7/20$ $P(\chi^2) = 61\%$ $CL = 46\%$
2π (only angular)	$\chi^2/\text{DOF} = 6.6/14$ $P(\chi^2) = 95\%$ $CL = 27\%$	$\chi^2/\text{DOF} = 19.6/12$ $P(\chi^2) = 7.6\%$ $CL < 0.1\%$

TABLE II: Results of the Toy MC

hypothesis at 23% C.L., while conversely the $X \rightarrow J/\psi \pi^+ \pi^- \pi^0$ data (third row) favor the 2^{-+} at 81% and exclude the 1^{++} hypothesis at 99.9% C.L. The two samples return therefore inconsistent answers.

Finally, in order to compare directly with Ref. [5] we report in Tab. II also the results performed using exclusively the two invariant mass distributions or the three angular distributions. Also here the former give a clear indication in favor of the 2^{-+} hypothesis, the latter in favor of the 1^{++} hypothesis. The different conclusion with respect to Ref. [5] comes both from a different theoretical model and from the appropriate treatment of the degrees of freedom with no sensitivity to the spin of the X .

V. CONCLUSIONS

We re-analyzed the $X \rightarrow J/\psi \pi^+ \pi^- \pi^0$ and $X \rightarrow J/\psi \pi^+ \pi^-$ invariant mass and angle distributions published by the Belle [2] and BaBar [1] collaborations respectively, with the goal to extract the most information about the spin of the X particle.

With respect to the existing analyzes, we have improved two aspects. On one side, the X decay amplitudes are parameterized by effective strong couplings, weighting terms written as products of momenta and polarizations as dictated by Lorentz invariance, and parity considerations in a model independent way. The strong couplings are given a momentum dependency according to the model defined in Eq. (7). This requires the introduction of an additional parameter R which can be related to the finite size of hadrons in the interaction region. The results, shown in Tab. I, are consistent with R of the order of 1 fm. The treatment is fully relativistic and particularly appropriate for angular analyses.

On the other side, in order to properly account for the sensitivities to the X spin of the considered distributions, we pursue a statistical approach based on Monte Carlo simulations.

We performed *i)* a global fit based on the whole information available from the 2π , 3π invariant mass spectra and the angular distributions of the $X \rightarrow J/\psi \rho$ decays, *ii)* two separated fits relative to the channels $J/\psi \rho$ (where we do the combined fit of the angular and invariant mass distributions) and $J/\psi \omega$ (fitting only the invariant mass distribution). We also studied the fit to the invariant mass and the angular distributions separately.

The combined fit *i)* excludes the 2^{-+} hypothesis at 99.9% C.L., but returns a probability of only 5.5% of the 1^{++} hypothesis being correct. The separate fits *ii)*, return a clear preference for the 1^{++} hypothesis in the $J/\psi \rho$ channel with a probability of 23% and an 81% preference for the 2^{-+} assignment in the $J/\psi \omega$ channel,

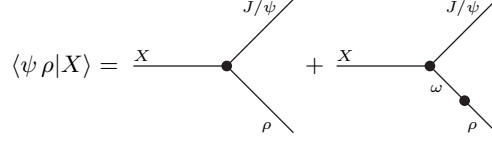


FIG. 6: Feynman diagrams of $X \rightarrow J/\psi \rho$ including the ρ - ω mixing. The second diagram includes the coupling ϵ and the propagator of the ω .

with very strong exclusions of other hypotheses. Such results go in the direction of two different assignments for the two samples, which can lead to a host of interesting considerations.

Acknowledgements

We would like to thank F.C. Porter for the discussion on the statistical approach, and F. Renga for the analysis of experimental data about the width of the X . We also wish to thank C. Sabelli for her collaboration in the early stages of this work. The work of F. P. was supported by the Research Executive Agency (REA) of the European Union under the Grant Agreement number PITN-GA-2010-264564 (LHCPhenoNet).

Appendix A: ρ - ω mixing

As discussed in Sec. III, the isospin-violating ρ - ω mixing introduces a correction near the pole of the ω , without affecting the core of our analysis. Moreover, we found that the mixing improves the quality of the fit of 2^{-+} and worsens the 1^{++} .

First of all, we have to insert the mixing into (10) and (14). Following Ref. [5], we describe the decay $\omega \rightarrow 2\pi$, as the oscillation $\omega \rightarrow \rho \rightarrow 2\pi$, as explained in Fig. 6. We call $-\epsilon$ the coupling of the vertex $\rho\omega$, whose value can be extracted by [5, 13]:

$$\epsilon \approx \sqrt{m_\omega m_\rho \Gamma_\rho \Gamma_\omega \mathcal{BR}(\omega \rightarrow 2\pi)} \approx 3.4 \cdot 10^{-3} \text{ GeV}^2 \quad (\text{A1})$$

The choice to treat the mixing reproduces naturally the phase of 95° of the complex mixing parameter used in Ref. [2].

Under the hypothesis 1^{++} we have

$$\langle \psi \rho(q) | X \rangle = g_{1\psi\rho} T - \epsilon g_{1\psi\omega} \frac{1}{q^2 - m_\omega^2 + im_\omega \Gamma_\omega} T \quad (\text{A2})$$

where T is the S-wave scalar described in (1). Similarly for 2^{-+}

$$\langle \psi \rho(q) | X \rangle = (g_{2\psi\rho} T_A + g'_{2\psi\rho} T_B) - \epsilon \frac{g_{2\psi\omega} T_A + g'_{2\psi\omega} T_B}{q^2 - m_\omega^2 + im_\omega \Gamma_\omega} \quad (\text{A3})$$

We can repeat the same argument for $\langle \psi \omega(q) | X \rangle$ by swapping the role of ρ and ω . The rest of Eqs. (13) and (17) (namely the Breit-Wigner and the decay into pions) is unchanged, because in this picture it is only the ρ (resp. the ω) which can decay in 2π (3π), being the mixing exhausted in the $\langle \psi V | X \rangle$ matrix element.

Moreover, if we take the mixing into account, the parameters $r_{J\rho}$ and $r_{J\omega}$ of the fit appear together in both channels; therefore we must impose their correct relative normalization. This can be solved by imposing that $\Gamma(X \rightarrow J/\psi 3\pi) / \Gamma(X \rightarrow J/\psi 2\pi) = 0.8 \pm 0.3$ [1, 8].

The angular distributions are unaffected by this term since they depend exclusively on the spin of the particles involved and not on the invariant mass spectrum. Therefore, to show the impact of the ρ - ω mixing we perform fits to the $m_{2\pi}$ and $m_{3\pi}$ distributions including this effect. The results are shown in Fig. 7, with the individual components detailed for the $m_{2\pi}$ distribution in Fig. 8. The resulting values of the radii vary from $R_1 = 1.6 \pm 0.3$ to $R_1 = 1.1 \pm 0.4$ and from $R_2 = 5.6 \pm 0.8$ to $R_2 = 4.5 \pm 0.7$. As far as the hypothesis testing is concerned

the χ^2/DOF changes from 25.2/22 to 29.3/22 for the 1^{++} hypothesis, and from 17.7/20 to 16.0/20 for the 2^{-+} one. None of the relevant conclusions is altered by this small effect and we will therefore neglect it in the main analysis.

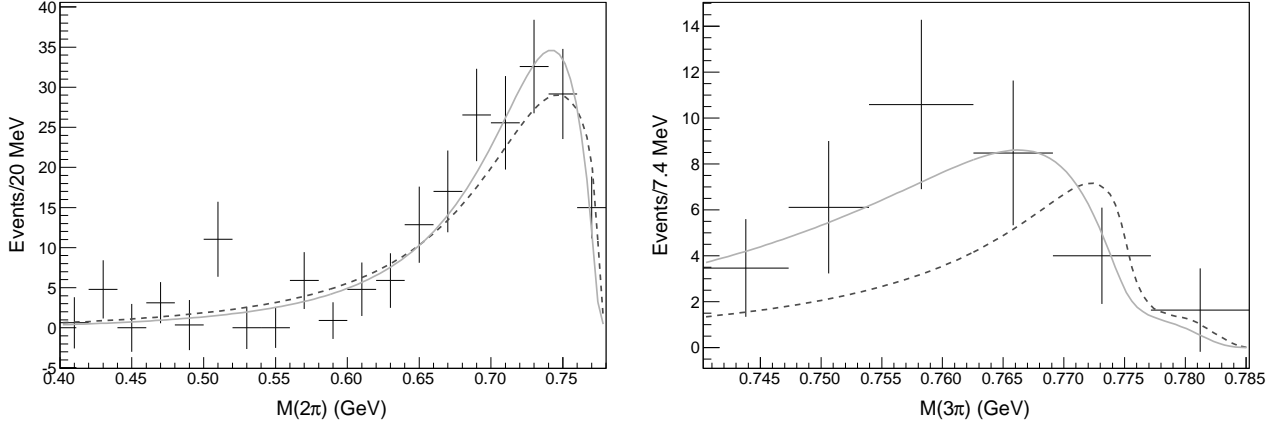


FIG. 7: Fit including ρ - ω mixing to the $m_{2\pi}$ (left) and $m_{3\pi}$ (right) distributions, with the model with $n = 1$. The dashed curve refers to the 1^{++} hypothesis, the solid one to the 2^{-+} one.

One could have thought that the presence of the narrow propagator of the ω would have constrained the fit to raise a peak at $m_\omega = 782$ MeV. The smallness of ϵ , instead, does not allow this, and the curve stays smooth at the pole, coherently with Refs. [2, 5, 6].

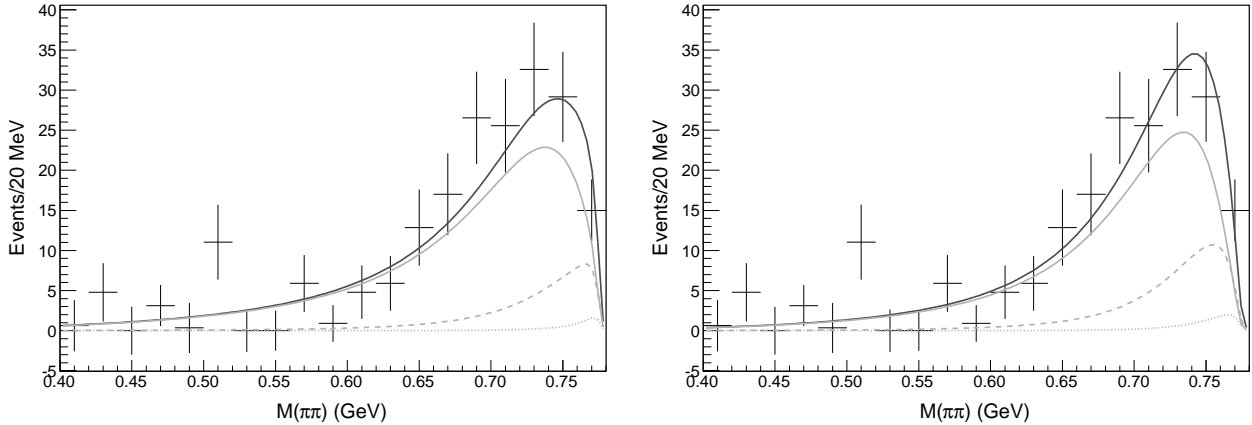


FIG. 8: Fit to the $m_{2\pi}$ distribution including ρ - ω mixing, with the model with $n = 1$, and under the hypothesis $J^{PC} = 1^{++}$ (left) and 2^{-+} (right). The solid light curve is the ρ contribution to the fit; the dotted light curve is the ω contribution, and the dashed curve is the interference term. The darker curve is the sum of all contributions.

Appendix B: $n = 2$ case

The theoretical model chosen for the fits described in this paper does not specify the value of n in Eq. (7), and it is therefore a free parameter of the model itself. Before adopting $n = 1$ for the rest of our considerations, we have performed a check on the dependence of the results on the choice of n .

Since the angular distributions have shown a scarce dependence on R , we fitted the invariant mass spectra with $n = 2$ comparing the result with the $n = 1$ case. The results are shown in Fig. 9. The resulting values of the radii vary from $R_1 = 1.6 \pm 0.3$ to $R_1 = 1.1 \pm 0.2$ and from $R_2 = 5.6 \pm 0.8$ to $R_2 = 2.8 \pm 0.3$. As far as the hypothesis testing is concerned the χ^2/DOF changes from 25.2/22 to 24.8/22 for the 1^{++} hypothesis, and from 17.7/20 to 18.9/20 for the 2^{-+} one. Also in this case none of the relevant conclusions is altered.

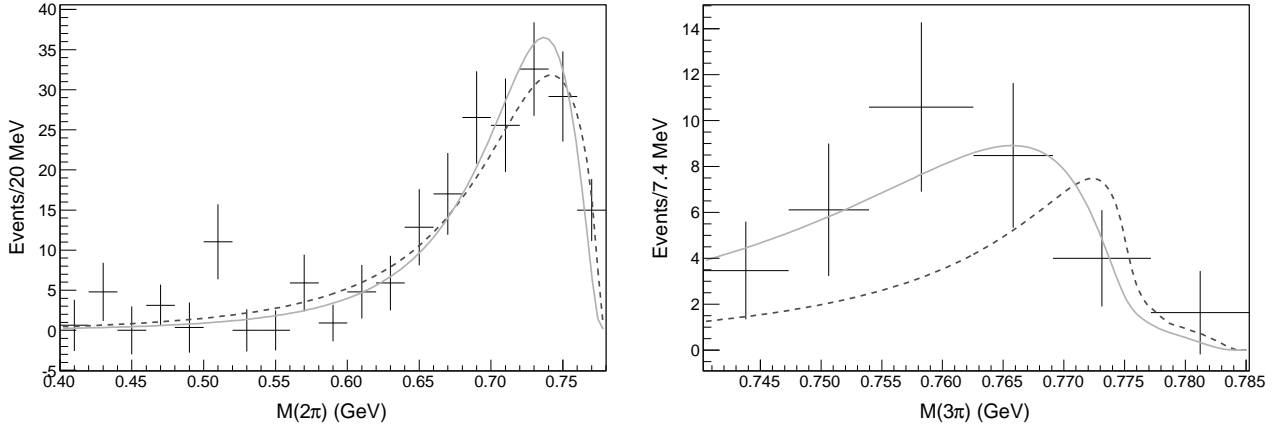


FIG. 9: Fit to the $m_{2\pi}$ (left) and $m_{3\pi}$ (right) distributions as described in the text, with the model with $n = 2$. The dashed curve refers to the 1^{++} hypothesis, the solid one is for the 2^{-+} one.

-
- [1] P. del Amo Sanchez *et al.* [BABAR Collaboration], Phys. Rev. D **82** (2010) 011101 [[arXiv:1005.5190 \[hep-ex\]](#)].
 - [2] S.-K. Choi, S. L. Olsen, K. Trabelsi, I. Adachi, H. Aihara, K. Arinstein, D. M. Asner and T. Aushev *et al.*, Phys. Rev. D **84** (2011) 052004 [[arXiv:1107.0163 \[hep-ex\]](#)].
 - [3] A. Abulencia *et al.* [CDF Collaboration], Phys. Rev. Lett. **98** (2007) 132002 [[arXiv:hep-ex/0612053](#)].
 - [4] F. Brazzi, B. Grinstein, F. Piccinini, A. D. Polosa and C. Sabelli, Phys. Rev. D **84** (2011) 014003 [[arXiv:1103.3155 \[hep-ph\]](#)].
 - [5] C. Hanhart, Y. S. Kalashnikova, A. E. Kudryavtsev and A. V. Nefediev, Phys. Rev. D **85** (2012) 011501 [[arXiv:1111.6241 \[hep-ph\]](#)].
 - [6] A. Abulencia *et al.* [CDF Collaboration], Phys. Rev. Lett. **96** (2006) 102002 [[arXiv:hep-ex/0512074](#)]. [[hep-ex/0512074](#)].
 - [7] J. L. Rosner, Phys. Rev. D **70** (2004) 094023 [[arXiv:hep-ph/0408334](#)].
 - [8] N. Drenska, R. Faccini, F. Piccinini, A.D. Polosa, F. Renga and C. Sabelli, Riv. Nuovo Cim. **033**, 633 (2010) [[arXiv:1006.2741 \[hep-ph\]](#)].
 - [9] E. Braaten and M. Kusunoki, Phys. Rev. D **69**, 074005 (2004) [[arXiv:hep-ph/0311147](#)]. S. Pakvasa and M. Suzuki, Phys. Lett. B **579**, 67 (2004) [[arXiv:hep-ph/0309294](#)]. M. B. Voloshin, Phys. Lett. B **579**, 316 (2004) [[arXiv:hep-ph/0309307](#)]. M. B. Voloshin, Phys. Lett. B **604**, 69 (2004) [[arXiv:hep-ph/0408321](#)].
 - [10] C. Bignamini, B. Grinstein, F. Piccinini, A. D. Polosa and C. Sabelli, Phys. Rev. Lett. **103**, 162001 (2009) [[arXiv:0906.0882 \[hep-ph\]](#)].
 - [11] P. Artoisenet and E. Braaten, Phys. Rev. D **81** (2010) 114018 [[arXiv:0911.2016 \[hep-ph\]](#)].
 - [12] L. Demortier, “P values and nuisance parameters”, into L. Lyons, (ed.), H. B. Prosper, (ed.) and A. De Roeck, (ed.), “Statistical issues for LHC physics. Proceedings, Workshop, PHYSTAT-LHC, Geneva, Switzerland, June 27-29, 2007”, [<http://phystat-lhc.web.cern.ch/phystat-lhc/proceedings.html>]
 - [13] H. B. O’Connell, B. C. Pearce, A. W. Thomas and A. G. Williams, Prog. Part. Nucl. Phys. **39** (1997) 201 [[arXiv:hep-ph/9501251](#)].